

1-D Three Phase Lag Bio-heat Model for Targeted Hyperthermia Treatment in Multiple Skin Layers

Solana Fernandez¹ and Andrew Carpino¹

¹Department of Bioengineering, University of California, San Diego, 3223 Voigt Dr., La Jolla, 92093, CA, USA.

August 5, 2025

Abstract

Accurate prediction of temperature fields is critical for safe and effective hyperthermia. Based off of a single layer model, our one-dimensional three phase lag bio-heat model treats skin as three distinct layers; epidermis, dermis and subcutaneous fat. We used a targeted Gaussian heat source at tumor depth rather than at the skin surface boundary. Beyond the standard metabolic and perfusion terms, our model adds vaporization and diffusive heat components, creating a more complete representation of how energy moves and dissipates in living tissue during therapy.

1 Introduction

Hyperthermia and thermal ablation therapies are widely used in oncology to selectively destroy tumor tissue with heat while minimizing collateral damage to healthy tissue. The effectiveness of these techniques hinges on our ability to predict and control temperature distributions within living tissue, and thus the accuracy of mathematical bioheat transfer models. The foundational model in this area is the Pennes [2] bioheat equation, which treats tissue as a homogeneous medium and assumes heat propagation via classical Fourier’s law [1]. While influential, this model has important limitations, including the nonphysical assumption of infinite thermal propagation speed, which can lead to significant discrepancies when simulating rapid thermal events such as those encountered during hyperthermia or ablation.

To address the shortcomings of the Pennes and classical Fourier models, Cattaneo [2] and Vernotte [3] introduced the concept of thermal relaxation, leading to the single phase lag (SPL) model, which accounts for a finite delay between heat flux and temperature gradient changes. Tzou further advanced this work with the dual phase lag (DPL) model, introducing two separate relaxation times; one for the heat flux and one for the temperature gradient—thereby more realistically capturing the lagging behavior of heat conduction in biological tissues [4, 5]. Although the DPL model improved temporal accuracy, it still could not capture all aspects of non-Fourier heat conduction, particularly in tissues with complex structure, heterogeneity, and multi-scale transport phenomena. This led to the development of the three phase lag (TPL) model [6], which incorporates an additional relaxation time associated with thermal displacement. The TPL framework has shown enhanced predictive power in modeling non-equilibrium thermal processes in tissue, especially in situations with high-intensity, short-duration heating or cooling, such as in modern ablation and cryosurgical procedures.

While previous works on DPL and TPL models offered important theoretical insights, most have been restricted to either homogeneous (single-layer) tissue or to boundary conditions representing heat applied to the tissue surface [6], conditions that do not always match clinical scenarios. In reality, human skin comprises multiple layers (epidermis, dermis, subcutaneous fat) with distinct thermal properties and biological functions. Recent numerical studies have begun to incorporate multi-layer skin models, demonstrating that such structure can critically influence both the temperature distribution and the extent of tissue damage during hyperthermia [5]. Furthermore, traditional models often apply either Dirichlet (fixed temperature), Neumann (fixed heat flux), or Robin (convective) boundary conditions at the skin surface. However, hyperthermia devices in clinical practice frequently deliver energy directly and locally, such as by focused ultrasound or lasers, resulting in a spatially localized, often Gaussian-distributed, heat source within the tissue, rather than simply at its boundary. Recent literature highlights the necessity of modeling such targeted sources to more accurately reflect clinical treatments [5]. In addition to external heating, other internal heat sources, such as metabolic activity, blood perfusion, and vaporization (evaporative cooling), play significant roles in the temperature field and thus in tissue damage or survival. Incorporating all these terms is crucial for developing truly predictive models.

Despite advances in both mathematical rigor and computational methods, few studies have fully bridged the gap between theoretical models and the real clinical context—where tissue structure is layered, external heat source is targeted, and multiple physiological phenomena (diffusion, perfusion, metabolism, vaporization) act concurrently. This integration is critical for improving the safety and efficacy of hyperthermia treatments, guiding device design, and personalizing therapy to patient-specific anatomy and pathology.

Recent numerical implementations have shown that including multiple skin layers, realistic boundary conditions, and localized heat sources produces temperature profiles that better match experimental and clinical outcomes. For example, implementing a Gaussian-distributed heat source captures the focused effect of energy deposition by hyperthermia devices, as opposed to the non-physiological scenario of heating propagating inward from the surface. Similarly, explicit inclusion of vaporization and perfusion terms is important for capturing tissue responses under high-intensity heating and for predicting cooling effects from sweat or tissue vaporization, especially in highly vascular or metabolically active regions.

The aim of this project is to develop and implement a one-dimensional, three phase lag (TPL) bioheat model for hyperthermia and heat ablation, explicitly incorporating three skin layers (epidermis, dermis, subcutaneous fat) and a Gaussian-distributed external heat source to realistically simulate a focused hyperthermia device. The model also integrates all key physiological and physical heat sources and sinks, including diffusion, blood perfusion, metabolic heat production, and vaporization, to provide a comprehensive and predictive framework for temperature distribution in living tissue under therapeutic heating.

2 Baseline Model

The three-phase-lag (TPL) bio-heat formulation introduced by Kumar & Kaur [6] we will treat here as our baseline description of heat transfer during hyperthermia. Their model represents a single, homogeneous block of skin initially at core body temperature and subsequently exposed to an external thermal load applied at the tissue surface. Within that framework they incorporate the following:

- **Finite-speed heat conduction via three relaxation times;** one for heat flux, one for the temperature gradient, and one for thermal displacement, so the model overcomes the infinite-propagation limitation of standard Fourier conduction.
- **Physiological heat sources and sinks;** metabolic heat generation, and blood-perfusion exchange with arterial blood held at a fixed core temperature.
- **Surface-only energy delivery;** implemented through one of three classical boundary types (fixed surface temperature, fixed surface flux, or convective exchange), where the opposite face of the slab is treated as adiabatic, mimicking symmetry or insulation.
- **Uniform material properties throughout the skin;** a single value each for thermal conductivity, density, and specific heat.

Kumar & Kaur express temperature, space, time, and material parameters in dimensionless form, then solve the resulting problem numerically. Their procedure couples a finite-difference discretization in space with a Legendre-wavelet Galerkin expansion in time for time marching while retaining the higher-order time derivatives introduced by the lag terms. The resulting temperature profiles show how changing a lag time, the perfusion rate, or the metabolic rate alters the transient temperature field inside the slab. Because the heat load is applied only at the surface and the slab is homogeneous, internal temperature evolution is driven solely by conduction and perfusion from that boundary inward.

This model explores a 2-D finite domain, using a hybrid approach of finite difference method (FDM) and Legendre Wavelet Galerkin Method (LWGM). FDM using the central differencing method for the second spatial derivative efficiently handles the spatial grid and complex boundary conditions. LWGM enables high-accuracy solutions and efficient handling of stiff systems, especially for time-dependent problems with higher-order derivatives and phase lag effects. The system is then solved using the Bartels–Stewart algorithm.

2.1 Governing Equations

Heat transport in tissue is described here through a sequence of constitutive laws that culminate in the three-phase-lag (TPL) formulation adopted by Kumar & Kaur. Starting with standard Fourier law,

$$q = -k\nabla T \quad (1)$$

which links the heat-flux vector q to the spatial temperature gradient through the thermal conductivity k . Combining this with conservation of energy gives

$$\rho c \left(\frac{\partial T}{\partial t} \right) = -k\nabla q(r, t) + Q_{tot} \quad (2)$$

where ρ and cc are tissue density and specific heat, and Q_{tot} represents all volumetric sources and sinks (metabolic heat, perfusion, external heating, etc.). For finite speed heat transfer, Cattaneo and Vernotte [2] introduced a flux relaxation time τ_q , which introduces a delay between the formation of a temperature gradient and the resulting heat flux, yielding the single-phase-lag (SPL) law:

$$q(r, t + \tau_q) = -k\nabla T(r, t) \quad (3)$$

Tzou [4] extended this idea by adding a temperature-gradient relaxation time, τ_T , as a response of the temperature gradient to heat flux, producing the dual-phase-lag (DPL) form. This accounts for microstructural delays within tissue, such as in cells or capillaries:

$$q(r, t + \tau_q) = -k\nabla T(r, t + \tau_T) \quad (4)$$

Kumar & Kaur [6] further refined the model by including a third delay, τ_v , that represents a lag in the way thermal energy density shifts inside tissue; the resulting TPL constitutive law is as follows:

$$q(r, t + \tau_q) = k\nabla T(r, t + \tau_T) + k^* \frac{d}{dt} \nabla T(r, t_v) \quad (5)$$

These three τ parameters correct the non physical assumption of instant heat transfer found in Fourier-based models and allow for more accurate modeling of rapid or high-intensity thermal treatments. Solving for q from **Equation 5** and substituting into the local energy balance produces the governing TPL energy equation used throughout this work:

$$\left(1 + \tau_q \frac{d}{dt} \right) \left(\rho c \frac{\partial^2 T}{\partial t^2} - Q_{tot} \right) = \left(k^* + (k + k^* \tau_v) \frac{\partial}{\partial t} + k \tau_T \frac{\partial^2}{\partial t^2} \right) \left(\frac{\partial^2 T}{\partial r^2} \right) \quad (6)$$

The LHS multiplies the storage term and volumetric sources, embedding the heat-flux lag, while the RHS embeds both gradient and displacement lags. In the baseline model $Q_{tot} = Q_m + Q_b$, where Q_m is metabolic heat generation and $Q_b = \rho_b c_b w_b (T_b - T)$ represents blood-perfusion exchange. ρ_b , c_b , w_b , and T_b represent the density, specific heat, perfusion rate, and temperature of blood, respectively. These values are summarized in **Table 2**.

2.2 Initial and Boundary Conditions

Initial conditions of the baseline model are as follows, where T_0 is initial temperature of the tissue:

$$T(x, y, 0) = T_0 \quad (7)$$

$$\frac{\partial T(x, y, 0)}{\partial t} = 0 \quad (8)$$

$$\frac{\partial^2 T(x, y, 0)}{\partial t^2} = 0 \quad (9)$$

Boundary conditions (summarized in **Table 1**) can be expressed with

$$A_1 \frac{\partial T(0, y, t)}{\partial x} + B_1 T(0, y, t) = f_1(y, t)$$

where A_1, B_1 , and f_1 dictate the boundary type, and can be similarly applied in the y -dimension. Values were applied according to physical application: cryosurgery, ablation, ambient exchange, or insulated domains.

Boundary Conditions of First Kind (Dirichlet/Constant Temperature)

$$A_1 = 0, B_1 = 1, f_1(y, t) = T_w$$

where T_w is temperature at the boundary. This scenario applies to cryosurgery or cooling probe applications; laser/ablation devices with precision in temperature control.

Boundary Conditions of Second Kind (Neumann/Constant Heat Flux)

$$A_1 = -k, B_1 = 0, f_1(y, t) = q_w$$

where q_w is the specified flux. This may relate to heat ablation where a device delivers a constant heat flux (not fixed temperature) or high-intensity focused ultrasound or laser ablation scenarios where energy delivery is specified as a rate (W/m^2) rather than a fixed temperature. Moreover, $q_w = 0$ indicates perfect insulation, which may be ideal for an internal boundary, centerline of symmetry, or insulated boundary. This is often applied at the far edge (deep tissue, core) or mid-plane for symmetric models.

Boundary Conditions of Third Kind (Robin/Convective)

$$A_1 = -k, B_1 = h, f_1(y, t) = hT_p \quad (10)$$

with heat transfer coefficient, h , and reference temperature, T_p . This is perfect for convective cooling/heating (e.g., tissue in contact with air, water, or perfused blood vessels) and imitating physiological/realistic skin boundary - exchange with ambient air, immersion in fluid, or subdermal perfusion.

3 Improved Model Rationale

The baseline model in Kumar, M. et al. [6] shows finite-speed thermal waves and basic physiological heating/cooling, but it excludes two clinically important and two physiological realities that will be addressed in our improved formulation:

1. **Layered skin architecture;** epidermis, dermis, and subcutaneous fat each possess distinct conductivities, perfusion rates, and metabolic activity.
2. **Localized internal heating;** many modern hyperthermia devices deposit energy within the tissue rather than exclusively on the exterior surface.
3. **Effects of sweat evaporation;** On the skin surface (epidermis), heat is lost to the environment by water vaporization.
4. **Heat due to diffusion;** in all skin layers, there is an unaccounted-for heat loss due to water diffusion that depends on parameters intrinsic to each tissue type.

3.1 Mathematical Formulation

Our model adopts the TPL representation of Kumar, M. et al.'s bio-heat model in one dimension. Accordingly, after taking **Equation 5**, performing a first-order Taylor series expansion of each term and solving for $q(r, t)$, we yield **Equation 6**.

Like Kumar, M. et al., Q_{tot} represents the sum of all heat sources. However, where it previously consisted of the sum of perfusion and metabolic heat parameters (Q_b and Q_m , respectively), the improved model additionally considers water vaporization and diffusive heat (Q_v and Q_{d_i} , respectively):

$$Q_v = \frac{\Delta m \Delta H_{vap}}{\delta_c} \quad (11)$$

$$\Delta m = \frac{D_a M_w}{R_a} \left(\frac{P_w}{T_w} \right)_s \frac{RH}{\delta_c} \quad (12)$$

$$Q_{d_i} = \frac{D_{f_i} c_w (\rho_s - \rho_c)}{(\nabla r)^2} (T_i - T_{0_i}) \quad (13)$$

as well as a targeted, Gaussian distributed heat source, represented by Q_r :

$$Q_r = Q_{r_0} e^{-a_0(r-r^*)^2} \quad (14)$$

$$Q_{r_0} = \rho_i S P \quad (15)$$

Where Δm , ΔH_{vap} , and δ_c are the rate of water vaporization, the enthalpy of water vaporization, and average boundary layer difference, respectively. D_{f_i} , c_w , ρ_s , ρ_c , and ∇r are the diffusivity of water, water content on the layer skin, water content on the core body, and characteristic diffusion distance. S , P , a_0 , r , r^* are the antenna constant, power, scattering parameter, depth of location, and depth of the tumor. Optimized and empirical values can be found in **Table 2**.

Initial conditions were adopted from the original model (**Equations 7- 9**), where the first and second

Boundary Condition	Application/Scenario	Example
First Kind (Dirichlet)	Cryosurgery probe, fixed-temp ablation	Fixed probe at 100°C or −180°C
Second Kind (Neumann)	Fixed heat flux ablation, laser energy delivery	Laser delivering 5000 W/m ²
Third Kind (Robin/Convective)	Skin–air/water interface, convective boundary	Skin exposed to air ($h \approx 5\text{--}25$ W/m ² K)
Fourth Kind (Mixed Interface)*	Tissue–device/tumor–normal interface (advanced models)	Tumor boundary, prosthetic interface
Symmetry/Zero-Flux (Neumann)	Core boundary, centerline, deep insulation	Deep tissue, center symmetry

Table 1: Boundary Conditions in Kumar, M. et al. [6] and Their Physical Applications. *Not included in paper, but used in advanced implementations.

temporal derivatives of temperature are equal to zero at time zero. Additionally, initial temperature at time zero (T_0) throughout each layer of tissue is considered to be 37°C.

Boundary Conditions of Third Kind (Robin/Convective) were employed at either end:

$$-k \frac{\partial T}{\partial t} \Big|_{x=0|L} = h(T_{x=0|L} - T_{amb})$$

Accordingly, using a forward Euler approximation at the superficial end:

$$T(x=0, t) = \frac{(\Delta x h T_{amb}) + k_i T(\Delta x, t)}{\Delta x h + k_i} \quad (16)$$

and backward Euler approximation at the deep end:

$$T(x=L, t) = \frac{\Delta x h T_{amb} - k_i T(L - \Delta x, t)}{\Delta x h - k_i} \quad (17)$$

At the interface/shared boundaries of the epidermis, dermis, and subcutaneous tissues temperature and heat flux were maintained/equivalent.

Central differencing is used to achieve the second spatial derivative, and forward difference for the first time derivative. Higher-order time derivatives were approximated with a pseudo-identity due to their near-negligible effects:

$$\begin{aligned} \frac{\partial^2 T}{\partial x^2} &= \frac{T(x + \Delta x, t) + T(x - \Delta x, t) - 2T(x, t)}{\Delta x^2} \\ \frac{\partial T}{\partial t} &= \frac{T(x, t + \Delta t) - T(x, t)}{\Delta t} \\ \frac{\partial^2 T}{\partial t^2} &= \frac{k^* (\frac{\partial^2 T}{\partial x^2})}{\rho c} \end{aligned}$$

Which, when substituted into **Equation 6** and rearranged for $T(x, t + \Delta t)$ (or T_i^{n+1} in discretized form) yields the time update rule:

$$\begin{aligned} T_i^{n+1} = T_i^n + \Delta t \Bigg(& \frac{(k \frac{\partial^2 T}{\partial x^2} + Q_{tot})}{\rho_i c_i} + \\ & \frac{\tau_q (k \frac{\partial^2 T}{\partial x^2} + Q_{tot})}{\rho_i c_i} - \tau_T \frac{k^*}{\rho_i c_i} \frac{\partial^2 T}{\partial x^2} + \\ & (k + \tau_v k^*) \frac{(k \frac{\partial^2 T}{\partial x^2} + Q_{tot})}{\rho_i c_i} \Bigg) \quad (18) \end{aligned}$$

3.2 Implementation in MATLAB

Our improved model was executed in MATLAB using the time-step update step described by **Equation 18** for internal points, and the exterior nodes with **Equations 16-17**. Physical parameters, such as ρ_i , c_i , and others, were recovered from literature, and those that were unavailable (τ_q , τ_v , and τ_T) or are clinically tunable (P , S , and a_0) were optimized for our implementation. See empirical and optimized values in **Table 2**.

4 Results

After implementing the improvements to our model, we first assessed the influence of the three phase-lag parameters on the spatial temperature profile at $t = 10$ s (**Figure 1a**). Varying behaviors of the temperature profiles guided our selection of $[\tau_q, \tau_T, \tau_v] = [10, 20, 1]$. Next, we varied the applied power P of the Gaussian source Q_r from 10W to 50W and tuned P to 35W to achieve a maximum value of around 45 °C (**Figure 2a**), then adjusted the antenna constant a_0 to 1×10^6 to balance localization and peak temperature (**Figure 2b**). Finally, we observed the location of Q_r 's influence on the temperature distribution curve, entirely within the different layers and comparing the full model (with Q_v and Q_d) against different variations. We found that omitting Q_v or Q_d does not significantly change the curve for a tumor at $r^* = 8$ mm (**Figure 4a**).

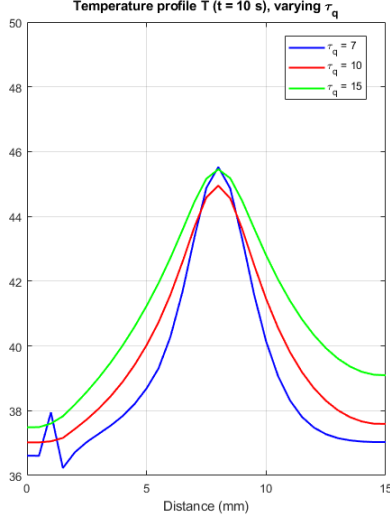
4.1 Varying Tau Parameters

To observe the differences in tau values, we generated temperature distributions over the distance into the skin with varying parameters. Each curve was generated at $t = 10$ seconds with default parameters equivalent to our original heat distribution. Default parameters for tau are 10, 20, and 1 for τ_q , τ_T , and τ_v , respectively. Results shown in **Figure 1**.

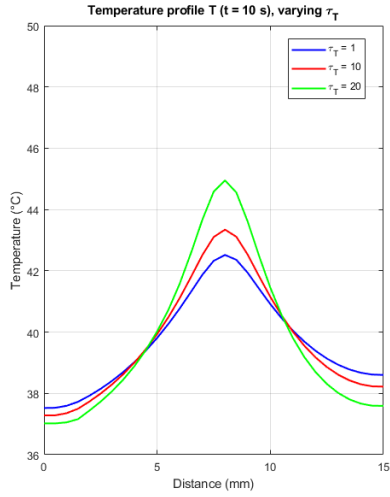
τ_Q : Values below 7 corrupt the model and temperature values are inconsistent. Values around 15 flatten out and also decrease localization of the heat too much; value of 10 was kept.

τ_T : Higher values tightened the heat distribution at the cost of exponentially increasing maximum temperature; we kept a value of 20 and tuned power P of the Q_r term (See **Table 2**) for an acceptable temp value. See [power section] for comparisons.

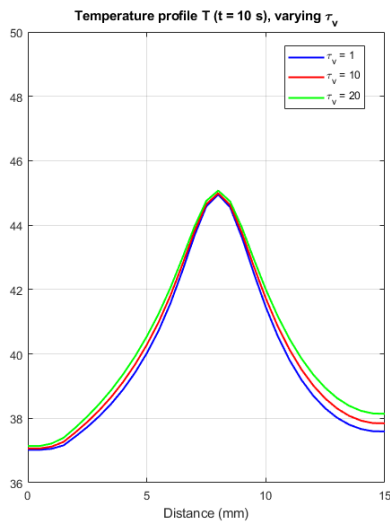
τ_V : Remained stable for increasing values, but increasing values decreased localization of the hyperthermia treatment. Minimizing τ_v value had best results.



(a)



(b)



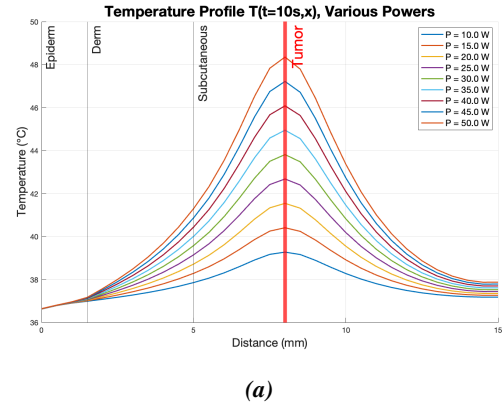
(c)

Figure 1: Altering τ_Q (a), τ_T (b), and τ_V (c) at $t = 10$ seconds and 35W in the multilayer model.

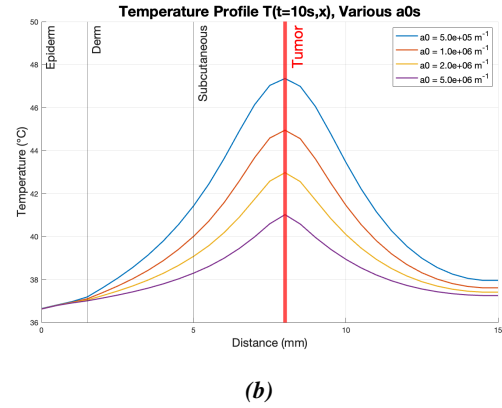
4.2 Varying Targeted Heat Source Parameters

To evaluate how external thermal energy influences spatial temperature profiles across multilayer skin tissue, we varied the power term P in our model. This analysis allowed us to examine how different levels of applied energy alter heat propagation and accumulation at the tumor site embedded within the subcutaneous layer.

The range of power inputs tested (10–50 W) reflects clinically realistic values used in localized hyperthermia. Sherlock and Crivelli [7] demonstrated that 60W of microwave energy applied for 30 minutes resulted in safe, tolerable heating of muscle tissue without irreversible thermal injury. This guided our selection of 50W as the upper bound, providing confidence that the modeled heating conditions are consistent with clinical tolerability.



(a)



(b)

Figure 2: Spatial profile of temperature at various powers (a) and various scattering parameters, a_0 (b).

As shown in **Figure 2a**, increasing power leads to greater temperature elevation within the tissue, with 35W producing a tumor-centered peak just above 45°C. This temperature falls within the optimal therapeutic hyperthermia range, as shown by Zahra et al. [8], who emphasized that temperatures exceeding 43°C reliably induce cancer cell death without compromising adjacent healthy tissue. This considers the tumor only in the subcutaneous layer; in the next section we discuss the effects of the skin layers and show how the wattage chosen in therapy varies based on the location of the

tumor.

Gaussian width control was also a factor in alteration of parameters. The antenna constant a_0 directly contributed to the spread of the heat source Q_r at the site of the tumor. Shown in **Figure 2b**, narrowing the source represented an ideal heat source and maintained a more localized heat distribution, however increased peak temperature to levels beyond our desired threshold. Finalizing a value of $1e6$ (**Table 2**) allowed for the proper temperature at a constant power of 35W determined previously.

4.3 Impact of Skin Layers & Heat Sources

We observed the impact of skin layers to be significant in both location of the tumor and overall heat distribution. Overall, accounting for heterogeneity of tissues (and therefore different values of ρ_i and c_i) results in a flattened spatial profile. This is consistent with the fact that the epidermis and dermis have larger and smaller specific heats, causing temperatures to be hotter and cooler under the same conditions in either tissue, respectively (**Figure 3**). Because the subcutaneous tissue in our model is predominant (10mm) and the tumor is located within this domain, subcutaneous homogeneity looks similar to our 3-layer model. However, when the subcutaneous tissue thickness changes (as it does throughout various locations of the human body and varies individual-to-individual) and the tumor moves locations, the spatial distribution of temperature is highly modulating. This variance demonstrates the need for precise measurements, targeting, and control of device heat source parameters in the clinical setting.

Exclusion of our additional heat sources Q_v and Q_d shows minimal effect on temperature profile for a tumor located at $r^* = 8mm$ within the subcutaneous tissue. However, when the tumor moves locations, such as into the dermis as seen in **Figure 4**, there is a more significant difference between our improved skin-layer TPL model and the baseline.

5 Discussion

In this work, we have presented a three-phase-lag bio-heat model for multilayered skin that captures important characteristics of hyperthermia treatment. By tuning the phase-lag delays, the power input, and the spread of the Gaussian heat source, we identified the key parameters influencing treatment localization and peak temperature. These findings highlight the critical role of parameter selection in designing safe and effective hyperthermia treatments. The ability to predict how changes in time lags, applied power, and source geometry affect internal heating has the potential for improving treatment options and planning.

Several different advancements can further enhance our model fidelity and clinical applicability. Incorporating heat-sink effects will improve predictions of temperature dynamics over longer treatment durations, and incorporating a feedback control system that ensures the tumor remains within the therapeutic temperature range will provide more realistic simulations. We also plan to investigate regional differences in skin thickness and

thermal properties based on location of the body. The largest extension of our model would be applying it into two- and three-dimensional geometries to capture complex tissue interfaces that are more biologically relevant.

6 Code Availability

MATLAB code for the mathematical model and for generating the figures and plots is available on GitHub: TPL_bioheat_model.

Scripts:

- `changing_tau_final.m`: Performs the analysis under 'Varying Tau Parameters'
- `a0_test_final.m` & `power_test_final.m`: Performs the analysis under 'Varying Targeted Heat Source Parameters'
- `skin_layer_comparison.m`: Performs the analysis under 'Impact of Skin Layers and Heat Sources'
- `main_final.m`: Runs the model with optimized parameters

References

- [1] Harry H Pennes. Analysis of tissue and arterial blood temperatures in the resting human forearm. *Journal of applied physiology*, 1(2):93–122, 1948.
- [2] Carlo Cattaneo. A form of heat-conduction equations which eliminates the paradox of instantaneous propagation. *Comptes rendus*, 247:431, 1958.
- [3] Pierre Vernotte. Les paradoxes de la theorie continue de l'equation de la chaleur. *Comptes rendus*, 246:3154, 1958.
- [4] Da Yu Tzou. *Macro-to microscale heat transfer: the lagging behavior*. John Wiley & Sons, 2014.
- [5] Tejaswini Kumari, Dinesh Kumar, KN Rai, and SK Singh. Numerical solution of dpl heat transfer model in multi-layer biological skin tissue of the living body during hyperthermia treatment. *Mechanics Based Design of Structures and Machines*, 51(1):159–178, 2023.
- [6] Mukesh Kumar, Subrahmanyam Upadhyay, Surjan Singh, KN Rai, et al. Mathematical modelling and simulation of three phase lag bio-heat transfer model during cancer treatment. *International Journal of Thermal Sciences*, 184:108002, 2023.
- [7] Noriko Ichinoseki-Sekine, Hisashi Naito, Norio Saga, Yuji Ogura, Minoru Shiraishi, Arrigo Giombini, Valentina Giovannini, and Shizuo Katamoto. Changes in muscle temperature induced by 434 mhz microwave hyperthermia. *British Journal of Sports Medicine*, 41(7):425–429, 2007.
- [8] Weiwei Zhu, Siwei Pan, Jiaqing Zhang, Jingli Xu, Ruolan Zhang, Yanqiang Zhang, Zhenjie Fu, Yuqi Wang, Can Hu, and Zhiyuan Xu. The role of hyperthermia in the treatment of tumor. *Critical Reviews in Oncology/Hematology*, page 104541, 2024.

Variable	Name	Units	Value	Reference
ρ_1	epidermis denisty	kg/m^3	1150	[9]
ρ_2	dermis density	kg/m^3	1116	[10]
ρ_3	subcutaneous density	kg/m^3	900	[11]
c_1	epidermis specific heat	$J/kg \cdot C$	3590	[12]
c_2	dermis specific heat	$J/kg \cdot C$	3330	[12]
c_3	subcutaneous specific heat	$J/kg \cdot C$	2500	[12]
L_1	thickness of epidermis	mm	1.5	[5]
L_2	thickness of dermis	mm	3.5	[5]
L_3	thickness of subcutaneous	mm	10	[5]
k_1	epidermis thermal conductivity	$W/m^\circ C$	0.2	[13]
k_2	dermis thermal conductivity	$W/m^\circ C$	0.45	[13]
k_3	subcutaneous thermal conductivity	$W/m^\circ C$	0.3	[13]
r^*	tumor depth/location	mm	0.8	**
P	transmitted power	W	35	[14]
S	antenna constant	1/kg	15	[14]
a_0	scattering parameter	m^{-1}	1e6	[14]
τ_T	relaxation time due to temperature gradient	s	20	[15] **
τ_v	relaxation time due to thermal displacement	s	1	[15] **
τ_q	relaxation time due to heat flux	s	10	[15] **
k^*	hyperbolic-term coefficient	$W/m^\circ C s$	0.1	*
h	convective coefficient at boundaries	$W/m^2 \circ C s$	4.5	[5]
w_b	blood perfusion rate	s^{-1}	0.8	[6]
ρ_b	density of blood	kg/m^3	1056	[5]
c_b	blood specific heat	$J/(kg^\circ C)$	4000	[5]
Q_{m_0}	metabolic heat baseline	W/m^3	50.65	[6]
T_b	arterial blood temperature	$^\circ C$	37	[6]
T_l	ambient/tissue temperature	$^\circ C$	37	[6]
D_a	average water vapor diffusivity	m^2/s	2.5e-5	[16]
M_w	molar mass of water	kg/mol	0.018	[17]
R_a	universal gas constant	$J/mol * K$	8.314	[17]
T_w	absolute temperature of skin surface	K	306	[18]
R_h	Relative Humidity	unit-less fraction	0.5	[19]
δ_c	average boundary layer difference	m	1e-4	[18]
c_{air}	specific heat of air	$J/kg^\circ C$	1005	[20]
D_f	diffusivity of water	m^2/s	2e-9	[21]
c_w	specific heat of water	$J/kg^\circ C$	4180	[5]
ρ_s	water content on the epidermis	kg/m^3	1100	[5]
ρ_c	water content on the core body	$J/kg^\circ C$	1000	[5]
$(\nabla r)^2$	characteristic distance squared	m^2	L_i^2	[5]

Table 2: A summary of the optimal parameters. (* An exact value could not be found within literature and was estimated. ** Variables changed and optimized throughout model development.)

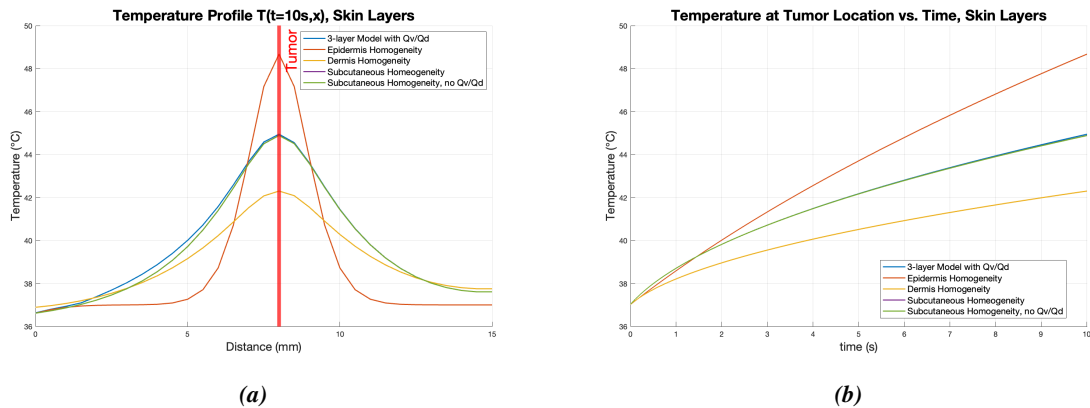


Figure 3: Spatial profile of temperature (a) and temperature at tumor location ($r^* = 8mm$) (b) considering the physical parameters of various skin layers. The green line considers subcutaneous homogeneity without the added heat sources of vaporization or diffusion.

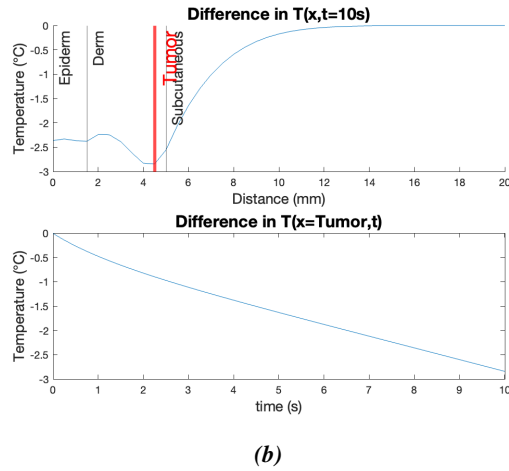
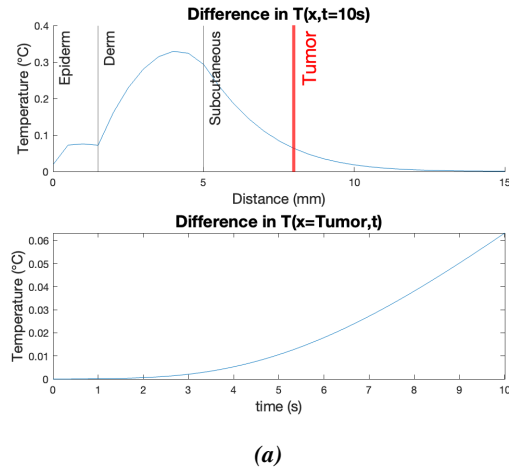


Figure 4: Difference between the improved model and baseline model (assuming subcutaneous homogeneity without Q_v or Q_d , but using the targeted heat source, Q_r) for the temperature profile at 10s and temperature at the tumor over time. Figure (a) illustrates $r^* = 8\text{mm}$ in the subcutaneous tissue and (b) is $r^* = 4.5\text{mm}$ in the dermis.

- [9] John Cameron. Physical properties of tissue. a comprehensive reference book, edited by Francis A. Duck, 1991.
- [10] Chunhui Li, Guangying Guan, Roberto Reif, Zhihong Huang, and Ruikang K Wang. Determining elastic properties of skin by measuring surface waves from an impulse mechanical stimulus using phase-sensitive optical coherence tomography. *Journal of The Royal Society Interface*, 9(70):831–841, 2012.
- [11] F Fidanza. Body fat in adult man: semicentenary of fat density and skinfolds. *Acta diabetologica*, 40:s242–s245, 2003.
- [12] Ming Fu, Wenguo Weng, and Hongyong Yuan. Numerical simulation of the effects of blood perfusion, water diffusion, and vaporization on the skin temperature and burn injuries. *Numerical Heat Transfer, Part A: Applications*, 65(12):1187–1203, 2014.
- [13] Zerin Jahan Tasnim and R Nasrin. Thermal wave and pennes’ models of bioheat transfer in human skin: A transient comparative analysis. *Heliyon*, 10(21), 2024.
- [14] Praveen Kumar Gupta, Jitendra Singh, Kabindra Nath Rai, and SK Rai. Solution of the heat transfer problem in tissues during hyperthermia by finite difference–decomposition method. *Applied Mathematics and Computation*, 219(12):6882–6892, 2013.
- [15] Dinesh Kumar, Surjan Singh, and KN Rai. Analysis of classical fourier, spl and dpl heat transfer model in biological tissues in presence of metabolic and external heat source. *Heat and Mass Transfer*, 52(6):1089–1107, 2016.
- [16] Charles V Paganelli and Fred K Kurata. Diffusion of water vapor in binary and ternary gas mixtures at increased pressures. *Respiration Physiology*, 30(1-2):15–26, 1977.
- [17] G.A. Truskey, F. Yuan, and D.F. Katz. *Transport Phenomena in Biological Systems*. Pearson Prentice Hall bioengineering. Pearson Prentice Hall, 2009.
- [18] Ming Fu, Wenguo Weng, and Hongyong Yuan. Numerical simulation of the effects of blood perfusion, water diffusion, and vaporization on the skin temperature and burn injuries. *Numerical Heat Transfer, Part A: Applications*, 65(12):1187–1203, 2014.
- [19] Nelson GC Astrath, Jun Shen, Datong Song, Jurandir H Rohling, Francine BG Astrath, Jianqin Zhou, Titichai Navessin, Zhong Sheng Liu, Caikang E Gu, and Xinsheng Zhao. The effect of relative humidity on binary gas diffusion. *The Journal of Physical Chemistry B*, 113(24):8369–8374, 2009.

-
- [20] Gases-Specific Heats and Individual Gas Constants. The engineering toolbox. *URL* https://www.engineeringtoolbox.com/specific-heat-capacity-water-d_660.html, 2004.
- [21] COMSOL Multiphysics Cyclopedia. Understanding the diffusion coefficient. *URL* <https://www.comsol.com/multiphysics/diffusion-coefficient>, 2017.

6.1 main_final.m

```

1
2 %
3
4 % main_final.m
5 % 1D hyperbolic bioheat w/ Gaussian tumor source, 3 skin layers, finer mesh
6 % and reduced dt for stability; snapshots at 2.5, 5, 7.5, 10 s in one plot.
7 %
8
9
10 %% 1) DISCRETIZE TIME & SPATIAL DOMAINS
11 % Skin Layer thickness
12 L_epi = 0.0015; % Epidermis (1.5 mm)
13 L_derm = 0.0035; % Dermis (3.5 mm)
14 L_subq = 0.01; % Subcutaneous (10 mm)
15 Lx = L_epi + L_derm + L_subq; % Domain Length
16
17 x_ast = 0.008; % [m] Tumor center (midpoint of 0.05 m)
18
19 dx = 0.0005; % [m] Spatial step now 21 nodes from 0 to 0.05
20 dt = 0.015; % [s] Time step (smaller for stability)
21 max_time = 10; % plot up to 10s
22 time_steps = round(max_time/dt) + 1; % ensures we reach exactly 10 s: (n 1)*dt =
23 10
24 time = 0:dt:max_time+dt;
25
26 x = 0:dx:Lx; % x = [0, 0.0025, 0.005, , 0.05]
27 nx = numel(x);
28
29 % Define Layers
30 layer = zeros(1, nx);
31 layer(x <= L_epi) = 1; % Epidermis
32 layer(x > L_epi & x <= L_epi + L_derm) = 2; % Dermis
33 layer(x > L_epi + L_derm) = 3; % Subcutaneous
34
35 % Find index of tumor center (closest grid point to x_ast)
36 [~, iTumor] = min(abs(x - x_ast));
37
38 %% 2) CONSTANTS AND PARAMETERS
39 % ----- Physical Parameters -----
40 % Skin Layer params
41 rho = [1150 1116 900]; % [kg/m^3] Tissue density (layers)
42 c = [3590 3300 2500]; % [J/(kg C)] Tissue specific heat
43 k = [0.2 0.45 0.3]; % [W/(m C)] Thermal conductivity
44 k_star = [0.1 0.1 0.1]; % [W/(m C s)] Hyperbolic term coefficient
45
46 % Blood params
47 h = 4.5; % [W/(m^2 C)] Convective coefficient at boundaries
48 wb = 0.0098; % [1/s] Blood perfusion
49 rho_b = 1056; % [kg/m^3] Blood density
50 cb = 4000; % [J/(kg C)] Blood specific heat
51
52 Qm0 = 50.65; % [W/m^3] Metabolic heat (uniform)
53 Tb = 37; % [C] Arterial blood temperature
54 Tl = [37 37 37]; % [C] Initial Ambient/tissue reference
55
56 % ----- Gaussian source parameters -----
57 % Q_r(i) = rho * S * P * exp( -a0*( x(i) - x_ast )^2 )
58 S = 15; % perkg scaling factor
59 P = 35; % power factor (tune as needed)
60 a0 = 1e6; % [1/m] Gaussian width control

```

```

61 % ----- Water vaporization and diffusion -----
62 Da = 2.5e-5; % m^2/s (air)
63 Mw = 0.018; % kg/mol
64 Ra = 8.314; % J/mol K
65 Tw = 306; % K (~33 C )
66 Pw = 5600; % Pa (sat. vapor pressure at 33 C )
67 RH = 0.5; % Relative humidity (fraction)
68 delta = 1e-4; % m
69 c_air = 1005; % J/kg K
70 Df = [2e-9 2e-9 2e-9]; % m^2/s
71 cw = 4180; % J/kg C
72 rho_s = 1100; % kg/m^3
73 rho_c = 1000; % kg/m^3
74 nabla_r2 = (Lx/3)^2;
75
76 % ----- Hyperbolic relaxation times -----
77 tau_q = 10; % [s]
78 tau_T = 20; % [s]
79 tau_v = 1; % [s]
80
81 %% 3) INITIALIZE STORAGE FOR SNAPSHOTS
82 % Snapshot times (in seconds) and their corresponding loop indices
83 snapshot_times = linspace(2,max_time,5); % [2.5, 5.0, 7.5, 10.0];
84 snap_idx = round(snapshot_times/dt) + 1;
85 % e.g., 2.5/0.01 = 250 +1 = 251 t = (251 1 ) * 0.01 = 2.50 s
86
87 T_snapshots = zeros(nx, numel(snapshot_times));
88 % Each column j holds T(x) at t = snapshot_times(j)
89
90 % Tumor temp array
91 T_tumor = zeros(1, time_steps);
92
93 % ----- Initialize temperature fields at t=0 -----
94 T = ones(nx,1);
95 T(find(layer == 1)) = Tl(1); T(find(layer == 2)) = Tl(2);
96 T(find(layer == 3)) = Tl(3);
97 T_new = T;
98 dTdt = zeros(nx,1);
99 d2Tdt2 = zeros(nx,1);
100
101 %% 4) TIME MARCHING LOOP
102 for n = 1:time_steps
103
104     % (a) Update interior nodes i=2:( n x 1 )
105     for i = 2:(nx-1)
106         L = layer(i);
107
108         % (b) Calculate Heat Source values for given spatial step
109         % Metabolic Heat Source:
110         Qm = Qm0 * (1 + (T(i) - Tl(L))/10); % [W/m^3] metabolic
111
112         % Water diffusion:
113         Qd = (Df(L) * cw * (rho_s - rho_c) / nabla_r2) * (T(i) - Tl(L));
114
115         % Blood Perfusion (dermis, subq):
116         if L > 1
117             Qb = wb * rho_b * cb * (Tb - Tl(L)); % [W/m^3] perfusion (constant)
118         else
119             Qb = 0;
120         end
121
122         % Water vaporization (epidermis only)
123         if L == 1
124             Delta_m = (Da*Mw/(Ra*Tw)) * (Pw/Tw) * RH/(delta*c_air);
125             Delta_Hvap = 2400e3; % J/kg
126             Qv = Delta_m * Delta_Hvap / (delta * c_air);

```

```

127     else
128         Qv = 0;
129     end
130
131     % Gaussian tumor heat source at node i:
132     Qr = rho(L) * S * P * exp( -a0 * (x(i) - x_ast)^2 );
133
134     % Add up all heat sources to consolidate
135     Q_tot = Qm + Qd + Qb + Qv + Qr;
136
137     % 2 n d spatial derivative (finite difference)
138     d2Tdx2 = (T(i+1) - 2*T(i) + T(i-1)) / dx^2;
139
140     % Hyperbolic bioheat terms:
141     dTdt(i) = (k(L)*d2Tdx2 + Q_tot) / (rho(L) * c(L));
142     d2Tdt2(i) = (k_star(L)*d2Tdx2) / (rho(L) * c(L));
143
144     % Update temperature at node i (eq. 7):
145     T_new(i) = T(i) + dt * ( ...
146         dTdt(i) + tau_q*dTdt(i) ...
147         - tau_T*d2Tdt2(i) ...
148         + (k(L) + k_star(L)*tau_v)*dTdt(i) );
149 end
150
151 % (c) Convective (Robin) BC at left boundary (i = 1):
152 % Forward Euler Approx dx/t
153 T_new(1) = (k(1) * T(2) + h*dx*22) / (h*dx + k(1)); % 22C is RT
154
155 % (d) Convective (Robin) BC at right boundary (i = nx):
156 % Backward Euler Approx dx/dt
157 T_new(nx) = (h*dx*37 - k(3) * T(end-1)) / (h*dx - k(3)); % 37C is body temp
158
159 % (e) Advance to next timestep
160 T = T_new;
161
162 % (f) If current t matches any snapshot index, store T(x)
163 idx_this = find(snap_idx == n);
164 if ~isempty(idx_this)
165     T_snapshots(:, idx_this) = T;
166 end
167
168 % (g) Store T at tumor location
169 T_tumor(n) = T_new(iTumor);
170 end
171
172 %% 5) PLOT ALL T(x) PROFILES IN A SINGLE FIGURE
173 figure('Position',[200,200,800,500]);
174 hold on;
175
176 colors = lines(numel(snapshot_times));
177 for j = 1:numel(snapshot_times)
178     plot(x*1000, T_snapshots(:,j), 'Color', colors(j,:), 'LineWidth',1.5, ...
179         'DisplayName', sprintf('t_=%%.1f_s', snapshot_times(j)));
180 end
181
182 ylim([36 50])
183 xlim([0 Lx*10^3])
184 xline(0, '-', {'Epiderm'}, 'HandleVisibility','off', 'FontSize',16)
185 xline((L_epi)*10^3, '-', {'Derm'}, 'HandleVisibility','off', 'FontSize',16)
186 xline((L_epi+L_derm)*10^3, '-', {'Subcutaneous'}, 'HandleVisibility','off', 'FontSize',
187     ,16)
188 xline(x_ast*10^3, '-r', {'Tumor'}, 'LineWidth',5, 'HandleVisibility','off', 'FontSize',
189     ,20)
190 xlabel('Distance_(mm)', 'FontSize',16);
191 ylabel('Temperature_( C )', 'FontSize',16);
192 title(['Temperature_Profile_T(t=10s,x),_Various_times'], 'FontSize',20);
193 legend('Location','northeast','FontSize',16);

```

```

192 grid on;
193 hold off;
194
195 %% 6. PLOT: TUMOR TEMPERATURE VS TIME
196 figure;
197 plot(time(1:length(T_tumor)), T_tumor, 'r', 'LineWidth', 2);
198 xlim([0 time(end)])
199 ylim([36 50])
200 xlabel('time_(s)','FontSize',16);
201 ylabel('Temperature_( C )','FontSize',16);
202 title('Temperature_at_Tumor_Location_vs._Time','FontSize',20);
203 grid on;

```

Listing 1: main_final.m

6.2 changing_tau_final.m

```

1 %
2 % 1D hyperbolic bioheat w/ Gaussian tumor source, 3 skin layers, finer mesh
3 % Computes T(x) at t=10 s for three different tau_T / tau_v / tau_q values.
4 % Then plots each triplet in a 1 3 subplot.
5 %
6
7 clear; clc;
8
9 %% 1) DISCRETIZE TIME & SPATIAL DOMAINS
10 % Skin Layer thicknesses
11 L_epi = 0.0015; % Epidermis (1.5 mm)
12 L_derm = 0.0035; % Dermis (3.5 mm)
13 L_subq = 0.01; % Subcutaneous (10 mm)
14 Lx = L_epi + L_derm + L_subq; % Total slab thickness (m)
15
16 x_ast = 0.008; % [m] Tumor center (8 mm from surface)
17
18 dx = 0.0005; % [m] spatial step (Lx/dx + 1) nodes
19 dt = 0.015; % [s] time step (for stability)
20 max_time = 10; % [s] we want solution at t=10 s
21 time_steps = round(max_time/dt) + 1; % ensures (time_steps-1)*dt 10
22 time = (0:(time_steps-1)) * dt;
23
24 x = 0:dx:Lx; % grid from 0 to Lx in steps of dx
25 nx = numel(x);
26
27 % Build a layer index for each x(i):
28 layer = zeros(1,nx);
29 layer(x <= L_epi) = 1; % Epidermis
30 layer(x > L_epi & x <= L_epi + L_derm) = 2; % Dermis
31 layer(x > L_epi + L_derm) = 3; % Subcutaneous
32
33 % Find the grid index closest to x_ast for tumor location tracking:
34 [~, iTumor] = min(abs(x - x_ast));
35
36 %% 2) CONSTANTS AND PARAMETERS (unchanged except s )
37 % Physical parameters per layer:
38 rho = [1150, 1116, 900]; % [kg/m^3] densities for [epi, derm, subq]
39 c = [3590, 3300, 2500]; % [J/(kg C)] specific heats
40 k = [0.2, 0.45, 0.3]; % [W/(m C)] thermal conductivities
41 k_star = [0.1, 0.1, 0.1]; % [W/(m C s)] hyperbolic term coefficient
42
43 % Blood and convection:
44 h = 4.5; % [W/(m^2 C)] convective BC coefficient
45 wb = 0.0098; % [1/s] blood perfusion rate

```

```

46 rho_b = 1056;      % [kg/m^3] blood density
47 cb   = 4000;      % [J/(kg C)] blood specific heat
48
49 Qm0 = 50.65;      % [W/m^3] metabolic heat
50 Tb  = 37;         % [C] blood inlet temperature
51 Tl  = [37, 37, 37]; % [C] ambient/tissue reference for each layer
52 T0  = 37;         % [C] initial tissue temperature
53
54 % Gaussiansource parameters (same for all runs):
55 S    = 15;        % [unitless] perk g scaling
56 P    = 35;        % [unitless] power factor
57 a0   = 1e6;       % [1/m^2] Gaussian width control
58                      % Q_r(i) = rho(layer(i)) * S * P * exp(-a0*(x(i)-x_ast)^2)
59
60 %% 3) PREALLOCATE SNAPSHOT MATRICES
61 % Each finaltime profile has 3 columns, one for each tau value in that set:
62 T_tauT_snap = zeros(nx, 3);
63 T_tauV_snap = zeros(nx, 3);
64 T_tauQ_snap = zeros(nx, 3);
65
66 % We will hold the default values for the taus not being varied:
67 tauT_default = 20; % [s]
68 tauV_default = 1;  % [s]
69 tauQ_default = 10; % [s]
70
71 %% 4) VARY _T {2,3,4} (fix _v =1, _q =10)
72 tauT_list = [1, 10, 20]; % values over 25 begin to look unstable
73 for j = 1:3
74     tauT = tauT_list(j);
75     tau_v = tauV_default;
76     tau_q = tauQ_default;
77
78     % Initialize temperature fields at t=0:
79     T = ones(nx,1) * T0;
80     T_new = T;
81
82     % Time marching loop to t=10 s:
83     for n = 1:time_steps
84         for i = 2:(nx-1)
85             L = layer(i);
86
87             % 1) Metabolic heat (layer-dependent Tl):
88             Qm = Qm0 * (1 + (T(i) - Tl(L))/10);
89             % 2) Water diffusion (not varying here, same as original):
90             Da = 2.5e-5; Mw = 0.018; Ra = 8.314;
91             Tw = 306; Pw = 5600; RH = 0.5;
92             delta = 1e-4; c_air = 1005;
93             Df = [2e-9, 2e-9, 2e-9]; cw = 4180;
94             rho_s = 1100; rho_c = 1000; nabla_r2 = (Lx/3)^2;
95             Qd = (Df(L)*cw*(rho_s-rho_c)/nabla_r2)*(T(i)-Tl(L));
96
97             % 3) Perfusion (dermis+subq only):
98             if L > 1
99                 Qb = wb * rho_b * cb * (Tb - Tl(L));
100             else
101                 Qb = 0;
102             end
103
104             % 4) Vaporization (epidermis only):
105             if L == 1
106                 Delta_m = (Da*Mw/(Ra*Tw)) * (Pw/Tw) * RH/(delta*c_air);
107                 Delta_Hvap = 2400e3; % J/kg
108                 Qv = Delta_m * Delta_Hvap / (delta*c_air);
109             else
110                 Qv = 0;
111             end
112

```

```

113 % 5) Gaussian tumor source:
114 Qr = rho(L) * S * P * exp(-a0*(x(i)-x_ast)^2);
115
116 % 6) Sum all sources:
117 Q_tot = Qm + Qd + Qb + Qv + Qr;
118
119 % 7) Second derivative in x:
120 d2Tdx2 = (T(i+1) - 2*T(i) + T(i-1)) / dx^2;
121
122 % 8) Hyperbolic bioheat:
123 dTdt(i) = (k(L)*d2Tdx2 + Q_tot) / (rho(L)*c(L));
124 d2Tdt2(i) = (k_star(L)*d2Tdx2) / (rho(L)*c(L));
125
126 T_new(i) = T(i) + dt * ( ...
127     dTdt(i) + tau_q*dTdt(i) ...
128     - tau_T*d2Tdt2(i) ...
129     + (k(L) + k_star(L)*tau_v) * dTdt(i) );
130 end
131
132 % Convective BC at i=1 (left):
133 L = layer(1);
134 T_new(1) = (h*dx*Tl(L) + k(L)*T_new(2)) / (h*dx + k(L));
135 % Convective BC at i=nx (right):
136 L = layer(nx);
137 T_new(nx) = (h*dx*Tl(L) + k(L)*T_new(nx-1)) / (h*dx + k(L));
138
139 % Advance:
140 T = T_new;
141 end
142
143 % After 10 s, store the final profile in column j:
144 T_tauT_snap(:,j) = T;
145 end
146
147 %% 5) VARY _v {1,2,3} (fix _T =2, _q =10)
148 tauV_list = [1, 10, 20]; % minimizing works best
149 for j = 1:3
150     tau_T = tauT_default;
151     tau_v = tauV_list(j);
152     tau_q = tauQ_default;
153
154     % Initialize:
155     T = ones(nx,1) * T0;
156     T_new = T;
157
158     for n = 1:time_steps
159         for i = 2:(nx-1)
160             L = layer(i);
161
162             % (Same source calculations as above)
163             Qm = Qm0 * (1 + (T(i) - Tl(L))/10);
164             Da = 2.5e-5; Mw = 0.018; Ra = 8.314;
165             Tw = 306; Pw = 5600; RH = 0.5;
166             delta = 1e-4; c_air = 1005;
167             Df = [2e-9, 2e-9, 2e-9]; cw = 4180;
168             rho_s = 1100; rho_c = 1000; nabla_r2 = (Lx/3)^2;
169             Qd = (Df(L)*cw*(rho_s - rho_c)/nabla_r2)*(T(i) - Tl(L));
170
171             if L > 1
172                 Qb = wb * rho_b * cb * (Tb - Tl(L));
173             else
174                 Qb = 0;
175             end
176
177             if L == 1
178                 Delta_m = (Da*Mw/(Ra*Tw)) * (Pw/Tw) * RH/(delta*c_air);
179                 Delta_Hvap = 2400e3;

```

```

180         Qv          = Delta_m * Delta_Hvap / (delta*c_air);
181     else
182         Qv = 0;
183     end
184
185     Qr = rho(L) * S * P * exp(-a0*(x(i) - x_ast)^2);
186     Q_tot = Qm + Qd + Qb + Qv + Qr;
187
188     d2Tdx2 = (T(i+1) - 2*T(i) + T(i-1)) / dx^2;
189     dTdt(i) = (k(L)*d2Tdx2 + Q_tot) / (rho(L)*c(L));
190     d2Tdt2(i) = (k_star(L)*d2Tdx2) / (rho(L)*c(L));
191
192     T_new(i) = T(i) + dt * ( ...
193         dTdt(i) + tau_q*dTdt(i) ...
194         - tau_T*d2Tdt2(i) ...
195         + (k(L) + k_star(L)*tau_v) * dTdt(i) );
196     end
197
198     % BCs at i=1 and i=nx:
199     L = layer(1);
200     T_new(1) = (h*dx*Tl(L) + k(L)*T_new(2)) / (h*dx + k(L));
201     L = layer(nx);
202     T_new(nx) = (h*dx*Tl(L) + k(L)*T_new(nx-1)) / (h*dx + k(L));
203
204     T = T_new;
205 end
206
207 T_tauV_snap(:,j) = T;
208 end
209
210 %% 6) VARY _q {5,10,15} (fix _T =2, _v =1)
211 tauQ_list = [7, 10, 15]; % below 8, unstable -- above 15, localization decreases
212 for j = 1:3
213     tau_T = tauT_default;
214     tau_v = tauV_default;
215     tau_q = tauQ_list(j);
216
217     T = ones(nx,1) * T0;
218     T_new = T;
219
220     for n = 1:time_steps
221         for i = 2:(nx-1)
222             L = layer(i);
223
224             Qm = Qm0 * (1 + (T(i) - Tl(L))/10);
225             Da = 2.5e-5; Mw = 0.018; Ra = 8.314;
226             Tw = 306; Pw = 5600; RH = 0.5;
227             delta = 1e-4; c_air = 1005;
228             Df = [2e-9, 2e-9, 2e-9]; cw = 4180;
229             rho_s = 1100; rho_c = 1000; nabla_r2 = (Lx/3)^2;
230             Qd = (Df(L)*cw*(rho_s - rho_c)/nabla_r2)*(T(i)-Tl(L));
231
232             if L > 1
233                 Qb = wb * rho_b * cb * (Tb - Tl(L));
234             else
235                 Qb = 0;
236             end
237
238             if L == 1
239                 Delta_m = (Da*Mw/(Ra*Tw)) * (Pw/Tw) * RH/(delta*c_air);
240                 Delta_Hvap = 2400e3;
241                 Qv = Delta_m * Delta_Hvap / (delta*c_air);
242             else
243                 Qv = 0;
244             end
245
246             Qr = rho(L) * S * P * exp(-a0*(x(i)-x_ast)^2);

```



```

247     Q_tot = Qm + Qd + Qb + Qv + Qr;
248
249     d2Tdx2 = (T(i+1) - 2*T(i) + T(i-1)) / dx^2;
250     dTdt(i) = (k(L)*d2Tdx2 + Q_tot) / (rho(L)*c(L));
251     d2Tdt2(i) = (k_star(L)*d2Tdx2) / (rho(L)*c(L));
252
253     T_new(i) = T(i) + dt * ( ...
254         dTdt(i) + tau_q*dTdt(i) ...
255         - tau_T*d2Tdt2(i) ...
256         + (k(L) + k_star(L)*tau_v) * dTdt(i) );
257 end
258
259 % BCs:
260 L = layer(1);
261 T_new(1) = (h*dx*Tl(L) + k(L)*T_new(2)) / (h*dx + k(L));
262 L = layer(nx);
263 T_new(nx) = (h*dx*Tl(L) + k(L)*T_new(nx-1)) / (h*dx + k(L));
264
265 T = T_new;
266 end
267
268 T_tauQ_snap(:,j) = T;
269 end
270
271 %% 7) PLOT ALL THREE SETS IN A SINGLE 1 3 SUBPLOT FIGURE
272 figure('Position',[200,200,1200,400]);
273
274 % 7.1) Subplot #1: varying tau_T
275 subplot(1,3,1);
276 plot(x*1000, T_tauT_snap(:,1), 'b', 'LineWidth',1.5); hold on;
277 plot(x*1000, T_tauT_snap(:,2), 'r', 'LineWidth',1.5);
278 plot(x*1000, T_tauT_snap(:,3), 'g', 'LineWidth',1.5);
279 ylim([36 50]);
280 xlabel('Distance_(mm)');
281 ylabel('Temperature_( C )');
282 title('Temperature_profile_T_\tau=\tau_10_s, \tau_varying_\tau_T');
283 legend('\tau_T=\tau_1', '\tau_T=\tau_10', '\tau_T=\tau_20', 'Location', 'best');
284 grid on;
285 hold off;
286
287 % 7.2) Subplot #2: varying tau_v
288 subplot(1,3,2);
289 plot(x*1000, T_tauV_snap(:,1), 'b', 'LineWidth',1.5); hold on;
290 plot(x*1000, T_tauV_snap(:,2), 'r', 'LineWidth',1.5);
291 plot(x*1000, T_tauV_snap(:,3), 'g', 'LineWidth',1.5);
292 ylim([36 50]);
293 xlabel('Distance_(mm)');
294 title('Temperature_profile_T_\tau=\tau_10_s, \tau_varying_\tau_v');
295 legend('\tau_v=\tau_1', '\tau_v=\tau_10', '\tau_v=\tau_20', 'Location', 'best');
296 grid on;
297 hold off;
298
299 % 7.3) Subplot #3: varying tau_q
300 subplot(1,3,3);
301 plot(x*1000, T_tauQ_snap(:,1), 'b', 'LineWidth',1.5); hold on;
302 plot(x*1000, T_tauQ_snap(:,2), 'r', 'LineWidth',1.5);
303 plot(x*1000, T_tauQ_snap(:,3), 'g', 'LineWidth',1.5);
304 ylim([36 50]);
305 xlabel('Distance_(mm)');
306 title('Temperature_profile_T_\tau=\tau_10_s, \tau_varying_\tau_q');
307 legend('\tau_q=\tau_7', '\tau_q=\tau_10', '\tau_q=\tau_15', 'Location', 'best');
308 grid on;
309 hold off;

```

Listing 2: changing_tau_final.m

6.3 a0_test_final

```

1 %
2 % a0_test_final.m
3 % 1D hyperbolic bioheat w/ Gaussian tumor source, 3 skin layers, finer mesh
4 % and reduced dt for stability; Varying a0 to find optimal parameter
5 %
6
7 clear; clc;
8
9 %% 1) DISCRETIZE TIME & SPATIAL DOMAINS
10 % Skin Layer thickness
11 L_epi = 0.0015; % Epidermis (1.5 mm)
12 L_derm = 0.0035; % Dermis (3.5 mm)
13 L_subq = 0.01; % Subcutaneous (10 mm)
14 Lx = L_epi + L_derm + L_subq; % Domain Length
15
16 x_ast = 0.008; % [m] Tumor center (midpoint of 0.05 m)
17
18 dx = 0.0005; % [m] Spatial step now 21 nodes from 0 to 0.05
19 dt = 0.015; % [s] Time step (smaller for stability)
20 max_time = 10; % plot up to 10s
21 time_steps = round(max_time/dt) + 1; % ensures we reach exactly 10 s: ( n 1 ) * dt =
    10
22 time = 0:dt:max_time+dt;
23
24 x = 0:dx:Lx; % x = [0, 0.0025, 0.005, , 0.05]
25 nx = numel(x);
26
27 % Define Layers
28 layer = zeros(1, nx);
29 layer(x <= L_epi) = 1; % Epidermis
30 layer(x > L_epi & x <= L_epi + L_derm) = 2; % Dermis
31 layer(x > L_epi + L_derm) = 3; % Subcutaneous
32
33 % Find index of tumor center (closest grid point to x_ast)
34 [~, iTumor] = min(abs(x - x_ast));
35
36 %% 2) CONSTANTS AND PARAMETERS
37 % ----- Physical Parameters -----
38 % Skin Layer params
39 rho = [1150 1116 900]; % [kg/m^3] Tissue density (layers)
40 c = [3590 3300 2500]; % [J/(kg C)] Tissue specific heat
41 k = [0.2 0.45 0.3]; % [W/(m C)] Thermal conductivity
42 k_star = [0.1 0.1 0.1]; % [W/(m C s)] Hyperbolic term coefficient
43
44 % Blood params
45 h = 4.5; % [W/(m^2 C)] Convective coefficient at boundaries
46 wb = 0.0098; % [1/s] Blood perfusion
47 rho_b = 1056; % [kg/m^3] Blood density
48 cb = 4000; % [J/(kg C)] Blood specific heat
49
50 Qm0 = 50.65; % [W/m^3] Metabolic heat (uniform)
51 Tb = 37; % [C] Arterial blood temperature
52 Tl = [37 37 37]; % [C] Initial Ambient/tissue reference
53
54 % ----- Gaussian source parameters -----
55 % Q_r(i) = rho * S * P * exp( -a0*( x(i) - x_ast )^2 )
56 S = 15; % perkg scaling factor
57 P = 35; % power factor (tune as needed)
58 % a0 = 1e6; % [1/m] Gaussian width control
59
60 % ----- Water vaporization and diffusion -----

```

```

61 Da = 2.5e-5;      % m^2/s (air)
62 Mw = 0.018;      % kg/mol
63 Ra = 8.314;      % J/mol K
64 Tw = 306;        % K (~33 C )
65 Pw = 5600;        % Pa (sat. vapor pressure at 33 C )
66 RH = 0.5;         % Relative humidity (fraction)
67 delta = 1e-4;     % m
68 c_air = 1005;     % J/kg K
69 Df = [2e-9 2e-9 2e-9]; % m^2/s
70 cw = 4180;        % J/kg C
71 rho_s = 1100;     % kg/m^3
72 rho_c = 1000;     % kg/m^3
73 nabla_r2 = (Lx/3)^2;
74
75 % ----- Hyperbolic relaxation times -----
76 tau_q = 10;       % [s]
77 tau_T = 20;       % [s]
78 tau_v = 1;        % [s]
79
80
81 %% 3) INITIALIZE STORAGE FOR     SNAPSHOTS
82 % Snapshot times (in seconds) and their corresponding loop indices
83 snapshot_times = linspace(2,max_time,5); % [2.5, 5.0, 7.5, 10.0];
84 snap_idx = round(snapshot_times/dt) + 1;
85 % e.g., 2.5/0.01 = 250      +1 = 251      t = (251 1 )*0.01 = 2.50 s
86
87 T_a0 = zeros(nx,4); % For storing T(x,t=10s) for a0 testing
88 T_tumor_a0 = zeros(time_steps,4); % for storing tumor temp for a0 testing
89
90 z = 1;
91 a0s = [5e5 1e6 2e6 5e6]
92 for a0 = a0s
93     T_snapshots = zeros(nx, numel(snapshot_times));
94     % Each column j holds T(x) at t = snapshot_times(j)
95
96     % Tumor temp array
97     T_tumor = zeros(1, time_steps);
98
99     % ----- Initialize temperature fields at t=0 -----
100     T = ones(nx,1);
101     T(find(layer == 1)) = Tl(1); T(find(layer == 2)) = Tl(2);
102     T(find(layer == 3)) = Tl(3);
103     T_new = T;
104     dTdt = zeros(nx,1);
105     d2Tdt2 = zeros(nx,1);
106
107
108     %% 4) TIME MARCHING LOOP
109     for n = 1:time_steps
110
111         % (a) Update interior nodes i=2:( n x 1 )
112         for i = 2:(nx-1)
113             L = layer(i);
114
115             % (b) Calculate Heat Source values for given spatial step
116             % Metabolic Heat Source:
117             Qm = Qm0 * (1 + (T(i) - Tl(L))/10); % [W/m^3] metabolic
118
119             % Water diffusion:
120             Qd = (Df(L) * cw * (rho_s - rho_c) / nabla_r2) * (T(i) - Tl(L));
121
122             % Blood Perfusion (dermis, subq):
123             if L > 1
124                 Qb = wb * rho_b * cb * (Tb - Tl(L)); % [W/m^3] perfusion (
125                 % constant)
126             else
127                 Qb = 0;

```

```

127     end
128
129     % Water vaporization (epidermis only)
130     if L == 1
131         Delta_m = (Da*Mw/(Ra*Tw)) * (Pw/Tw) * RH/(delta*c_air);
132         Delta_Hvap = 2400e3; % J/kg
133         Qv = Delta_m * Delta_Hvap / (delta * c_air);
134     else
135         Qv = 0;
136     end
137
138     % Gaussian tumor heat source at node i:
139     Qr = rho(L) * S * P * exp( -a0 * (x(i) - x_ast)^2 );
140
141     % Add up all heat sources to consolidate
142     Q_tot = Qm + Qd + Qb + Qv + Qr;
143
144     % 2 n d spatial derivative (finite difference)
145     d2Tdx2 = (T(i+1) - 2*T(i) + T(i-1)) / dx^2;
146
147     % Hyperbolic bioheat terms:
148     dTdt(i) = (k(L)*d2Tdx2 + Q_tot) / (rho(L) * c(L));
149     d2Tdt2(i) = (k_star(L)*d2Tdx2) / (rho(L) * c(L));
150
151     % Update temperature at node i (eq. 7):
152     T_new(i) = T(i) + dt * ( ...
153         dTdt(i) + tau_q*dTdt(i) ...
154         - tau_T*d2Tdt2(i) ...
155         + (k(L) + k_star(L)*tau_v)*dTdt(i) );
156 end
157
158 % (c) Convective (Robin) BC at left boundary (i = 1):
159 % Forward Euler Approx dx/t
160 T_new(1) = (k(1) * T(2) + h*dx*22) / (h*dx + k(1)); % 22C is RT
161
162 % (d) Convective (Robin) BC at right boundary (i = nx):
163 % Backward Euler Approx dx/dt
164 T_new(nx) = (h*dx*37 - k(3) * T(end-1)) / (h*dx - k(3)); % 37C is body temp
165
166 % (e) Advance to next timestep
167 T = T_new;
168
169 % (f) If current t matches any snapshot index, store T(x)
170 idx_this = find(snap_idx == n);
171 if ~isempty(idx_this)
172     T_snapshots(:, idx_this) = T;
173 end
174
175 % (g) Store T at tumor location
176 T_tumor(n) = T_new(iTumor);
177 end
178
179 %% Store profile for given P to be compared after
180 T_a0(:,z) = T_snapshots(:,end);
181 T_tumor_a0(:,z) = T_tumor;
182 z = z+1;
183
184 end % end of testing parameter loop (power)
185
186 %% Plot T(x) for a0s
187 figure('Position',[200,200,800,500]);
188 hold on;
189
190 colors = lines(numel(a0s));
191 for j = 1:size(T_a0,2)
192     plot(x*1000, T_a0(:,j), 'Color', colors(j,:), 'LineWidth',1.5, ...
193         'DisplayName', sprintf('a0=%%.1e_m^-^1', a0s(j)));

```

```

194 end
195
196 ylim([36 50])
197 xlim([0 Lx*10^3])
198 xline(0, '-', {'Epiderm'}, 'HandleVisibility','off', 'FontSize',16)
199 xline((L_epi)*10^3, '-', {'Derm'}, 'HandleVisibility','off', 'FontSize',16)
200 xline((L_epi+L_derm)*10^3, '-', {'Subcutaneous'}, 'HandleVisibility','off', 'FontSize'
    ,16)
201 xline(x_ast*10^3, '-r', {'Tumor'}, 'LineWidth',5, 'HandleVisibility','off', 'FontSize'
    ,20)
202 xlabel('Distance_(mm)', 'FontSize',16);
203 ylabel('Temperature_( C )', 'FontSize',16);
204 title(['Temperature_Profile_T(t=10s,x),_Various_a0s'], 'FontSize',20);
205 legend('Location', 'northeast', 'FontSize',12);
206 grid on;
207 hold off;
208
209
210 %% 6. PLOT: TUMOR TEMPERATURE VS TIME
211 figure('Position', [200,200,800,500]);
212 hold on;
213
214 colors = lines(numel(a0s));
215 for j = 1:size(T_a0,2)
216     plot(time, T_tumor_a0(:,j), 'Color', colors(j,:), 'LineWidth',1.5, ...
217         'DisplayName', sprintf('a0_=%%.1e_m^-^1', a0s(j)));
218 end
219
220 xlim([0 time(end)])
221 ylim([36 50])
222 xlabel('time_(s)', 'FontSize',16);
223 ylabel('Temperature_( C )', 'FontSize',16);
224 title(['Temperature_at_Tumor_Location_vs._Time,_Various_a0s'], 'FontSize',20);
225 legend('Location', 'best', 'FontSize',12);
226 grid on;
227 hold off;

```

Listing 3: a0_test_final.m

6.4 power_test_final.m

```

1 %
2
3 % power_test_final.m
4 % 1D hyperbolic bioheat w/ Gaussian tumor source, 3 skin layers, finer mesh
5 % and reduced dt for stability; Varying Power to find optimal parameter
6 %
7
8
9 %% 1) DISCRETIZE TIME & SPATIAL DOMAINS
10 % Skin Layer thickness
11 L_epi = 0.0015; % Epidermis (1.5 mm)
12 L_derm = 0.0035; % Dermis (3.5 mm)
13 L_subq = 0.01; % Subcutaneous (10 mm)
14 Lx = L_epi + L_derm + L_subq; % Domain Length
15
16 x_ast = 0.008; % [m] Tumor center (midpoint of 0.05 m)
17
18 dx = 0.0005; % [m] Spatial step now 21 nodes from 0 to 0.05
19 dt = 0.015; % [s] Time step (smaller for stability)
20 max_time = 10; % plot up to 10s

```

```

21 time_steps = round(max_time/dt) + 1; % ensures we reach exactly 10 s: ( n 1 ) * dt =
    10
22 time = 0:dt:max_time+dt;
23
24 x = 0:dx:Lx; % x = [0, 0.0025, 0.005, , 0.05]
25 nx = numel(x);
26
27 % Define Layers
28 layer = zeros(1, nx);
29 layer(x <= L_epi) = 1; % Epidermis
30 layer(x > L_epi & x <= L_epi + L_derm) = 2; % Dermis
31 layer(x > L_epi + L_derm) = 3; % Subcutaneous
32
33 % Find index of tumor center (closest grid point to x_ast)
34 [~, iTumor] = min(abs(x - x_ast));
35
36 %% 2) CONSTANTS AND PARAMETERS
37 % ----- Physical Parameters -----
38 % Skin Layer params
39 rho = [1150 1116 900]; % [kg/m^3] Tissue density (layers)
40 c = [3590 3300 2500]; % [J/(kg C)] Tissue specific heat
41 k = [0.2 0.45 0.3]; % [W/(m C)] Thermal conductivity
42 k_star = [0.1 0.1 0.1]; % [W/(m C s)] Hyperbolic term coefficient
43
44 % Blood params
45 h = 4.5; % [W/(m^2 C )] Convective coefficient at boundaries
46 wb = 0.0098; % [1/s] Blood perfusion
47 rho_b = 1056; % [kg/m^3] Blood density
48 cb = 4000; % [J/(kg C)] Blood specific heat
49
50 Qm0 = 50.65; % [W/m^3] Metabolic heat (uniform)
51 Tb = 37; % [ C ] Arterial blood temperature
52 Tl = [37 37 37]; % [ C ] Initial Ambient/tissue reference
53
54 % ----- Gaussian source parameters -----
55 % Q_r(i) = rho * S * P * exp( -a0*( x(i) - x_ast )^2 )
56 S = 15; % perkg scaling factor
57 % P = 30; % power factor (tune as needed)
58 a0 = 1e6; % [1/m] Gaussian width control
59
60 % ----- Water vaporization and diffusion -----
61 Da = 2.5e-5; % m^2/s (air)
62 Mw = 0.018; % kg/mol
63 Ra = 8.314; % J/mol K
64 Tw = 306; % K (~33 C )
65 Pw = 5600; % Pa (sat. vapor pressure at 33 C )
66 RH = 0.5; % Relative humidity (fraction)
67 delta = 1e-4; % m
68 c_air = 1005; % J/kg K
69 Df = [2e-9 2e-9 2e-9]; % m^2/s
70 cw = 4180; % J/kg C
71 rho_s = 1100; % kg/m^3
72 rho_c = 1000; % kg/m^3
73 nabla_r2 = (Lx/3)^2;
74
75 % ----- Hyperbolic relaxation times -----
76 tau_q = 10; % [s]
77 tau_T = 20; % [s]
78 tau_v = 1; % [s]
79
80
81 %% 3) INITIALIZE STORAGE FOR SNAPSHOTS
82 % Snapshot times (in seconds) and their corresponding loop indices
83 snapshot_times = linspace(2,max_time,5); % [2.5, 5.0, 7.5, 10.0];
84 snap_idx = round(snapshot_times/dt) + 1;
85 % e.g., 2.5/0.01 = 250 +1 = 251 t = (251 1 ) * 0.01 = 2.50 s
86

```

```

87 T_p = zeros(nx,4); % For storing T(x,t=10s) for power testing
88 T_tumor_p = zeros(time_steps,4); % for storing tumor temp for power testing
89
90 z = 1;
91 powers = 10:5:50
92 for P = powers
93     T_snapshots = zeros(nx, numel(snapshot_times));
94     % Each column j holds T(x) at t = snapshot_times(j)
95
96     % Tumor temp array
97     T_tumor = zeros(1, time_steps);
98
99     % ----- Initialize temperature fields at t=0 -----
100     T = ones(nx,1) * Tl(1);
101     T(find(layer == 1)) = Tl(1); T(find(layer == 2)) = Tl(2);
102     T(find(layer == 3)) = Tl(3);
103     T_new = T;
104     dTdt = zeros(nx,1);
105     d2Tdt2 = zeros(nx,1);
106
107
108     %% 4) TIME MARCHING LOOP
109     for n = 1:time_steps
110
111         % (a) Update interior nodes i=2:( n x 1 )
112         for i = 2:(nx-1)
113             L = layer(i);
114
115             % (b) Calculate Heat Source values for given spatial step
116             % Metabolic Heat Source:
117             Qm = Qm0 * (1 + (T(i) - Tl(L))/10); % [W/m^3] metabolic
118
119             % Water diffusion:
120             Qd = (Df(L) * cw * (rho_s - rho_c) / nabla_r2) * (T(i) - Tl(L));
121
122             % Blood Perfusion (dermis, subq):
123             if L > 1
124                 Qb = wb * rho_b * cb * (Tb - Tl(L)); % [W/m^3] perfusion (
125                 % constant)
126             else
127                 Qb = 0;
128             end
129
130             % Water vaporization (epidermis only)
131             if L == 1
132                 Delta_m = (Da*Mw/(Ra*Tw)) * (Pw/Tw) * RH/(delta*c_air);
133                 Delta_Hvap = 2400e3; % J/kg
134                 Qv = Delta_m * Delta_Hvap / (delta * c_air);
135             else
136                 Qv = 0;
137             end
138
139             % Gaussian tumor heat source at node i:
140             Qr = rho(L) * S * P * exp( -a0 * (x(i) - x_ast)^2 );
141
142             % Add up all heat sources to consolidate
143             Q_tot = Qm + Qd + Qb + Qv + Qr;
144
145             % 2 n d spatial derivative (finite difference)
146             d2Tdx2 = (T(i+1) - 2*T(i) + T(i-1)) / dx^2;
147
148             % Hyperbolic bioheat terms:
149             dTdt(i) = (k(L)*d2Tdx2 + Q_tot) / (rho(L) * c(L));
150             d2Tdt2(i) = (k_star(L)*d2Tdx2) / (rho(L) * c(L));
151
152             % Update temperature at node i (eq. 7):
153             T_new(i) = T(i) + dt * ( ...

```

```

153         dTdt(i) + tau_q*dTdt(i) ...
154         - tau_T*d2Tdt2(i) ...
155         + (k(L) + k_star(L)*tau_v)*dTdt(i) );
156     end
157
158     % (c) Convective (Robin) BC at left boundary (i = 1):
159     % Forward Euler Approx dx/t
160     T_new(1) = (k(1) * T(2) + h*dx*22) / (h*dx + k(1)); % 22C is RT
161
162     % (d) Convective (Robin) BC at right boundary (i = nx):
163     % Backward Euler Approx dx/dt
164     T_new(nx) = (h*dx*37 - k(3) * T(end-1)) / (h*dx - k(3)); % 37C is body temp
165
166     % (e) Advance to next timestep
167     T = T_new;
168
169     % (f) If current t matches any snapshot index, store T(x)
170     idx_this = find(snap_idx == n);
171     if ~isempty(idx_this)
172         T_snapshots(:, idx_this) = T;
173     end
174
175     % (g) Store T at tumor location
176     T_tumor(n) = T_new(iTumor);
177 end
178
179 %% Store profile for given P to be compared after
180 T_p(:,z) = T_snapshots(:,end);
181 T_tumor_p(:,z) = T_tumor;
182 z = z+1;
183
184 end % end of testing parameter loop (power)
185
186 %% Plot T(x) for Powers
187 figure('Position',[200,200,800,500]);
188 hold on;
189
190 colors = lines(numel(powers));
191 for j = 1:size(T_p,2)
192     plot(x*1000, T_p(:,j), 'Color', colors(j,:), 'LineWidth',1.5, ...
193         'DisplayName', sprintf('P_=%%.1f_W', powers(j)));
194 end
195
196 ylim([36 50])
197 xlim([0 Lx*10^3])
198 xline(0, '-', {'Epiderm'}, 'HandleVisibility','off', 'FontSize',16)
199 xline((L_epi)*10^3, '-', {'Derm'}, 'HandleVisibility','off', 'FontSize',16)
200 xline((L_epi+L_derm)*10^3, '-', {'Subcutaneous'}, 'HandleVisibility','off', 'FontSize',
201     ,16)
202 xline(x_ast*10^3, '-r', {'Tumor'}, 'LineWidth',5, 'HandleVisibility','off', 'FontSize',
203     ,20)
204 xlabel('Distance_(mm)', 'FontSize',16);
205 ylabel('Temperature_( C )', 'FontSize',16);
206 title(['Temperature_Profile_T(t=10s,x),_Various_Powers'], 'FontSize',20);
207 legend('Location','northeast', 'FontSize',12);
208 grid on;
209 hold off;
210
211 %% 6. PLOT: TUMOR TEMPERATURE VS TIME
212 figure('Position',[200,200,800,500]);
213 hold on;
214
215 colors = lines(numel(powers));
216 for j = 1:size(T_p,2)
217     plot(time, T_tumor_p(:,j), 'Color', colors(j,:), 'LineWidth',1.5, ...
218         'DisplayName', sprintf('P_=%%.1f_W', powers(j)));

```



```

218 end
219
220 xlim([0 time(end)])
221 ylim([36 50])
222 xlabel('time_(s)','FontSize',16);
223 ylabel('Temperature_( C )','FontSize',16);
224 title(['Temperature_at_Tumor_Location_vs._Time,_Various_Powers'],'FontSize',20);
225 legend('Location','best','FontSize',12);
226 grid on;
227 hold off;

```

Listing 4: power_test_final.m

6.5 skin_layer_comparison.m

```

1 %
2 % 1D hyperbolic bioheat w/ Gaussian tumor source, 3 skin layers, finer mesh
3 % and reduced dt for stability; TESTING EFFECT OF SKIN LAYERS & HEAT
4 % SOURCES
5 %
6
7 clear; clc;
8
9 %% 1) DISCRETIZE TIME & SPATIAL DOMAINS
10 % Skin Layer thickness
11 L_epi = 0.0015; % Epidermis (1.5 mm)
12 L_derm = 0.0035; % Dermis (3.5 mm)
13 L_subq = 0.010; % Subcutaneous (10 mm)
14 Lx = L_epi + L_derm + L_subq; % Domain Length
15
16 x_ast = 0.008; % [m] Tumor center (midpoint of 0.05 m)
17
18 dx = 0.0005; % [m] Spatial step now 21 nodes from 0 to 0.05
19 dt = 0.015; % [s] Time step (smaller for stability)
20 max_time = 10; % plot up to 10s
21 time_steps = round(max_time/dt) + 1; % ensures we reach exactly 10 s: ( n 1 ) * dt =
    10
22 time = 0:dt:max_time+dt;
23
24 x = 0:dx:Lx; % x = [0, 0.0025, 0.005, , 0.05]
25 nx = numel(x);
26
27 % Define Layers
28 layer = zeros(1, nx);
29 layer(x <= L_epi) = 1; % Epidermis
30 layer(x > L_epi & x <= L_epi + L_derm) = 2; % Dermis
31 layer(x > L_epi + L_derm) = 3; % Subcutaneous
32
33 % Find index of tumor center (closest grid point to x_ast)
34 [~, iTumor] = min(abs(x - x_ast));
35
36 %% 2) CONSTANTS AND PARAMETERS
37 % ----- Physical Parameters -----
38 % Skin Layer params
39 % rho = [1150 1116 900]; % [kg/m^3] Tissue density (layers)
40 % c = [3590 3300 2500]; % [J/(kg C)] Tissue specific heat
41 % k = [0.2 0.45 0.3]; % [W/(m C)] Thermal conductivity
42 k_star = [0.1 0.1 0.1]; % [W/(m C s)] Hyperbolic term coefficient
43
44 % Blood params
45 h = 4.5; % [W/(m^2 C)] Convective coefficient at boundaries
46 wb = 0.0098; % [1/s] Blood perfusion

```

```

47 rho_b = 1056; % [kg/m^3] Blood density
48 cb = 4000; % [J/(kg C)] Blood specific heat
49
50 Qm0 = 50.65; % [W/m^3] Metabolic heat (uniform)
51 Tb = 37; % [C] Arterial blood temperature
52 Tl = [37 37 37]; % [C] Initial Ambient/tissue reference
53
54 % ----- Gaussian source parameters -----
55 % Q_r(i) = rho * S * P * exp( -a0*( x(i) - x_ast )^2 )
56 S = 15; % perkg scaling factor
57 P = 35; % power factor (tune as needed)
58 a0 = 1e6; % [1/m] Gaussian width control
59
60 % ----- Water vaporization and diffusion -----
61 Da = 2.5e-5; % m^2/s (air)
62 Mw = 0.018; % kg/mol
63 Ra = 8.314; % J/mol K
64 Tw = 306; % K (~33 C)
65 Pw = 5600; % Pa (sat. vapor pressure at 33 C)
66 RH = 0.5; % Relative humidity (fraction)
67 delta = 1e-4; % m
68 c_air = 1005; % J/kg K
69 Df = [2e-9 2e-9 2e-9]; % m^2/s?
70 cw = 4180; % J/kg C
71 rho_s = 1100; % kg/m^3
72 rho_c = 1000; % kg/m^3
73 nabla_r2 = (Lx/3)^2;
74
75 % ----- Hyperbolic relaxation times -----
76 tau_q = 10; % [s]
77 tau_T = 20; % [s]
78 tau_v = 1; % [s]
79
80
81 %% 3) INITIALIZE STORAGE FOR SNAPSHOTS
82 % Snapshot times (in seconds) and their corresponding loop indices
83 snapshot_times = linspace(2,max_time,5); % [2.5, 5.0, 7.5, 10.0];
84 snap_idx = round(snapshot_times/dt) + 1;
85 % e.g., 2.5/0.01 = 250 +1 = 251 t = (251 1)*0.01 = 2.50 s
86
87 T_layers = zeros(nx,5); % For storing T(x,t=10s) for layer testing
88 T_tumor_layers = zeros(time_steps,5); % for storing tumor temp for layer testing
89
90 for layer_test = 1:5
91
92     if layer_test == 1 % Heterogeneous case
93         rho = [1150 1116 900]; % [kg/m^3] Tissue density (layers)
94         c = [3590 3300 2500]; % [J/(kg C)] Tissue specific heat
95         k = [0.2 0.45 0.3]; % [W/(m C)] Thermal conductivity
96     elseif layer_test == 2 % Treat all as epidermis
97         rho = [1150 1150 1150]; % [kg/m^3] Tissue density (layers)
98         c = [3590 3590 3590]; % [J/(kg C)] Tissue specific heat
99         k = [0.2 0.2 0.2]; % [W/(m C)] Thermal conductivity
100    elseif layer_test == 3 % Treat all as dermis
101        rho = [1116 1116 1116]; % [kg/m^3] Tissue density (layers)
102        c = [3300 3300 3300]; % [J/(kg C)] Tissue specific heat
103        k = [0.45 0.45 0.45]; % [W/(m C)] Thermal conductivity
104    elseif layer_test == 4 | 5 % Treat all as subq
105        rho = [900 900 900]; % [kg/m^3] Tissue density (layers)
106        c = [2500 2500 2500]; % [J/(kg C)] Tissue specific heat
107        k = [0.3 0.3 0.3]; % [W/(m C)] Thermal conductivity
108    end
109
110    T_snapshots = zeros(nx, numel(snapshot_times));
111    % Each column j holds T(x) at t = snapshot_times(j)
112
113    % Tumor temp array

```

```

114 T_tumor = zeros(1, time_steps);
115
116 % ----- Initialize temperature fields at t=0 -----
117 T = ones(nx,1);
118 T(find(layer == 1)) = Tl(1); T(find(layer == 2)) = Tl(2);
119 T(find(layer == 3)) = Tl(3);
120 T_new = T;
121 dTdt = zeros(nx,1);
122 d2Tdt2 = zeros(nx,1);
123
124
125 %% 4) TIME MARCHING LOOP
126 for n = 1:time_steps
127
128     % (a) Update interior nodes i=2:( n x 1 )
129     for i = 2:(nx-1)
130         L = layer(i);
131
132         % (b) Calculate Heat Source values for given spatial step
133         % Metabolic Heat Source:
134         Qm = Qm0 * (1 + (T(i) - Tl(L))/10); % [W/m^3] metabolic
135
136         % Water diffusion:
137         Qd = (Df(L) * cw * (rho_s - rho_c) / nabla_r2) * (T(i) - Tl(L));
138
139         % Blood Perfusion (dermis, subq):
140         if L > 1
141             Qb = wb * rho_b * cb * (Tb - Tl(L)); % [W/m^3] perfusion (
142                 constant)
143         else
144             Qb = 0;
145         end
146
147         % Water vaporization (epidermis only)
148         if L == 1
149             Delta_m = (Da*Mw/(Ra*Tw)) * (Pw/Tw) * RH/(delta*c_air);
150             Delta_Hvap = 2400e3; % J/kg
151             Qv = Delta_m * Delta_Hvap / (delta * c_air);
152         else
153             Qv = 0;
154         end
155
156         % Gaussian tumor heat source at node i:
157         Qr = rho(L) * S * P * exp( -a0 * (x(i) - x_ast)^2 );
158
159         % Add up all heat sources to consolidate
160         if layer_test == 5
161             Qd = 0; Qv = 0;
162         end
163         Q_tot = Qm + Qd + Qb + Qv + Qr;
164
165         % 2 n d spatial derivative (finite difference)
166         d2Tdx2 = (T(i+1) - 2*T(i) + T(i-1)) / dx^2;
167
168         % Hyperbolic bioheat terms:
169         dTdt(i) = (k(L)*d2Tdx2 + Q_tot) / (rho(L) * c(L));
170         d2Tdt2(i) = (k_star(L)*d2Tdx2) / (rho(L) * c(L));
171
172         % Update temperature at node i (eq. 7):
173         T_new(i) = T(i) + dt * ( ...
174             dTdt(i) + tau_q*dTdt(i) ...
175             - tau_T*d2Tdt2(i) ...
176             + (k(L) + k_star(L)*tau_v)*dTdt(i) );
177     end
178
179     % (c) Convective (Robin) BC at left boundary (i = 1):
180     % Forward Euler Approx dx/t

```

```

180     T_new(1) = (k(1) * T(2) + h*dx*22) / (h*dx + k(1)); % 22C is RT
181
182     % (d) Convective (Robin) BC at right boundary (i = nx):
183     % Backward Euler Approx dx/dt
184     T_new(nx) = (h*dx*37 - k(3) * T(end-1)) / (h*dx - k(3)); % 37C is body temp
185
186     % (e) Advance to next timestep
187     T = T_new;
188
189     % (f) If current t matches any snapshot index, store T(x)
190     idx_this = find(snap_idx == n);
191     if ~isempty(idx_this)
192         T_snapshots(:, idx_this) = T;
193     end
194
195     % (g) Store T at tumor location
196     T_tumor(n) = T_new(iTumor);
197 end
198
199 %% Store profile for given P to be compared after
200 T_layers(:, layer_test) = T_snapshots(:, end);

```

```

201
202     T_tumor_layers(:, layer_test) = T_tumor;
203
204 end % end of testing parameter loop (power)
205
206 %% Plot T(x) for Layers
207 legend_layers = ["3-layer Model with Qv/Qd", "Epidermis Homogeneity", "Dermis
    Homogeneity", "Subcutaneous Homogeneity", "Subcutaneous Homogeneity, no Qv/Qd
    "];
208
209 figure('Position', [200, 200, 800, 500]);
210 hold on;
211
212 colors = lines(numel(legend_layers));
213 for j = 1:size(T_layers, 2)
214     plot(x*1000, T_layers(:, j), 'Color', colors(j, :), 'LineWidth', 1.5, ...
215         'DisplayName', num2str(legend_layers(j)));
216 end
217
218 ylim([36 50])
219 xlim([0 Lx*10^3])
220 % xline(0, '-', {'Epidermis'}, 'HandleVisibility', 'off', 'FontSize', 16)
221 % xline((L_epi)*10^3, '-', {'Dermis'}, 'HandleVisibility', 'off', 'FontSize', 16)
222 % xline((L_epi+L_dermi)*10^3, '-', {'Subcutaneous'}, 'HandleVisibility', 'off', 'FontSize
    ', 16)
223 xline(x_ast*10^3, '-r', {'Tumor'}, 'LineWidth', 5, 'HandleVisibility', 'off', 'FontSize'
    , 20)
224 xlabel('Distance_(mm)', 'FontSize', 16);
225 ylabel('Temperature_( C )', 'FontSize', 16);
226 title(['Temperature_Profile_T(t=10s,x),_Skin_Layers'], 'FontSize', 20);
227 legend('Location', 'northeast', 'FontSize', 12);
228 grid on;
229 hold off;
230
231
232 %% 6. PLOT: TUMOR TEMPERATURE VS TIME
233 figure('Position', [200, 200, 800, 500]);
234 hold on;
235
236 colors = lines(numel(legend_layers));
237 for j = 1:size(T_layers, 2)
238     plot(time, T_tumor_layers(:, j), 'Color', colors(j, :), 'LineWidth', 1.5, ...
239         'DisplayName', num2str(legend_layers(j)));
240 end
241

```

```

242 xlim([0 time(end)])
243 ylim([36 50])
244 xlabel('time_(s)','FontSize',16);
245 ylabel('Temperature_( C )','FontSize',16);
246 title(['Temperature_at_Tumor_Location_vs._Time,_Skin_Layers'],'FontSize',20);
247 legend('Location','best','FontSize',12);
248 grid on;
249 hold off;
250
251 T_layers_difference = T_layers(:,1)-T_layers(:,5);
252 T_tumor_layers_difference = T_tumor_layers(:,1)-T_tumor_layers(:,5);
253
254 figure
255 subplot(2,1,1)
256 hold on
257 plot(x*10^3,T_layers_difference)
258 xline(0, '-', {'Epiderm'}, 'HandleVisibility','off','FontSize',14)
259 xline((L_epi)*10^3, '-', {'Derm'}, 'HandleVisibility','off','FontSize',14)
260 xline((L_epi+L_derm)*10^3, '-', {'Subcutaneous'}, 'HandleVisibility','off','FontSize'
    ,14)
261 xline(x_last*10^3, '-r', {'Tumor'}, 'LineWidth',3,'HandleVisibility','off','FontSize'
    ,18)
262 title('Difference_in_T(x,t=10s)','FontSize',16)
263 xlabel('Distance_(mm)','FontSize',14);
264 ylabel('Temperature_( C )','FontSize',14);
265 hold off
266
267 subplot(2,1,2)
268 plot(time,T_tumor_layers_difference)
269 xlim([0 time(end)])
270 title('Difference_in_T(x=Tumor,t)','FontSize',16)
271 xlabel('time_(s)','FontSize',14);
272 ylabel('Temperature_( C )','FontSize',14);

```

Listing 5: skin.layer_comparison.m